Journal of Applied Polymer Science

Plugging properties and profile control effects of crosslinked polyacrylamide microspheres

Bo Wang,[1,2,3] Meiqin Lin,[1,3] Jinru Guo,[1,3] Dianlin Wang,[1,3] Fengqiang Xu,[1,3] Mingyuan Li[1,3]

[1]Enhanced Oil Recovery Research Institute, China University of Petroleum (Beijing), Fuxue Road 18,Changping, Beijing, 102249, China

[2]Liaoning Shihua University, Fushun, Liaoning, 113001, China

[3]Key Laboratory of Enhanced Oil Recovery, CNPC, Fuxue Road 18, Changping, Beijing, 102249, China

Correspondence to: M. Lin (E-mail: 13910509321@163.com)

ABSTRACT: In this article, the morphology, particle size, and plugging properties of crosslinked polyacrylamide (CPAM) microspheres were investigated through optical microscopy, scanning electron microscopy (SEM), nuclear-pore membrane filtration experiments, a micro-visual model, sandpack experiments, parallel twin-tube plugging, and oil displacement experiments. The results revealed that the primary particle sizes of the CPAM microspheres ranged from several hundreds of nanometers to 5 μm; however, after the microspheres were fully swelled in water, their sizes increased by approximately five times of their original sizes. As a CPAM microsphere dispersion system had good dispersibility and deformation capabilities, a 1.2 μm nuclear-pore membrane as well as the deep part of a sandpack tube could be effectively plugged. Consequently, the flow diversion effect was achieved in the vertical and planar directions. When the CPAM microspheres migrated in porous media, they could displace residual oil on the pole wall and water flow channel to realize the synchronization of profile control and coordination and improve recovery efficiency. © 2016 Wiley Periodicals, Inc. J. Appl. Polym. Sci. **2016**, *133*, 43666.

KEYWORDS: crosslinked polyacrylamide microsphere; swelling property; plugging effect; particle size; in-depth profile control

Received 17 November 2015; accepted 21 March 2016

DOI: 10.1002/app.43666

INTRODUCTION

Acrylamide-based polymers are widely used in oilfield development,[1–3] water treatment,[4,5] paper,[6] textiles, food, agriculture,[7] medicine,[8] and other basic fields and are indispensable to these fields. This is especially true for the oil and gas development field, in which acrylamide-based polymers are considered to be one of the earliest and most often used oil recovery agents due to their good water solubility, low concentration, ability to increase viscosity, and good selectivity.[9] However, the partial use of hydrolytic polyacrylamides (HPAM) is greatly limited in some respects because they undergo hydrolysis at high temperatures and exhibit poor salt resistance. Thus, they are not suitable for use in high temperature and high salinity oil reservoirs. Therefore, crosslinked gel particles (crosslinked polymer microspheres), which are prepared by copolymerizing acrylamide and other monomers, have been developed to enhance the salt tolerance of HPAM.[10,11]

The inverse emulsion polymerization method, which is used to prepare polyacrylamide (PAM) microspheres, not only solves the problems of high viscosity and the difficulty of removing polymerization heat by stirring for acrylamide polymers, but also has certain advantages, such as a high polymerization rate, a large molecular weight of the product, mild reaction conditions, and powdery or granular products can be obtained directly.[12] Furthermore, it is also a relatively mature technology and has been extensively applied. But industrialization is easily realized due to the simple process, the easy removal of polymerization heat, and the simple post-treatment.

The two most important factors of oil reservoir development are the sweep coefficient and oil displacement efficiency.[13,14] For a heterogeneous reservoir, the sweep coefficient is an important parameter for evaluating water flooding. It represents the spread of water flooding and affects the ultimate recoverable reserve and production of oil.[15,16] Therefore, enhancing the sweep coefficient and improving the heterogeneity of oil reservoirs are important issues. The principle of in-depth profile control and water shutoff uses plugging materials to allow flow to the deep part of the reservoir along with displacement fluid and block the high permeable channel, which leads to flow diversion such that the water flooding and volume are expanded. Specifically, excellent in-depth profile control and water shutoff materials

Table I. Twin-Tube Oil Displacement Experimental Results of the Microsphere Dispersion System

Sandpack tube	Permeability (μm^2)	Porosity (%)	Original contained oil saturation (%)	Oil displacement efficiency by water flooding (%)	Total oil displacement efficiency (%)	EOR %
High permeability	1.42	35.3	71.5	77	77.6	0.6
Low permeability	0.57	32.6	73.0	34	82.2	48.2

should have characteristics of "going in, blocking up, and transportation." An excellent candidate material for these applications is crosslinked polyacrylamide (CPAM) microspheres.[17] CPAM microspheres have certain advantages compared with HPAM, such as high molecular weight, controllable particle size, high water absorbency, anti-shearing, and applicability under harsh reservoir conditions.[18–22] In particular, the plugging properties and deformation capabilities of CPAM microspheres are both enhanced after the microspheres are swollen, which meets the basic requirements for the profile control of water materials.

At present, studies on the structure, particle size, and swelling characteristics of crosslinked polyacrylamide microspheres are relatively mature,[18,23,24] and there are some recent studies that have conducted research on the plugging properties of oil field depth profile control agents and their flow diversion effects. Yao *et al.* studied the selectivity, optimal matching factor, viscoelastic properties and microscopic flow and displacement mechanisms of pore-scale elastic microspheres and their use as a novel profile control and oil displacement agent.[25,26] Lin *et al.* studied the plugging mechanism of nanoscale polymer microspheres[23] and microspheres[27] (with sizes ranging from several microns to tens of microns) in porous media.

In this article, CPAM microspheres with sizes ranging from several hundreds of nanometers to 5 μm were synthesized and studied using a micro-visual model, nuclear-pore membrane filtration and sandpack experiments. By the means of three different plugging experiment models (from plane to stereoscopic), from macroscopic to microscopic scales, the plugging properties of CPAM microspheres on different profiles were studied, and their in-depth profile control mechanism was also proposed.

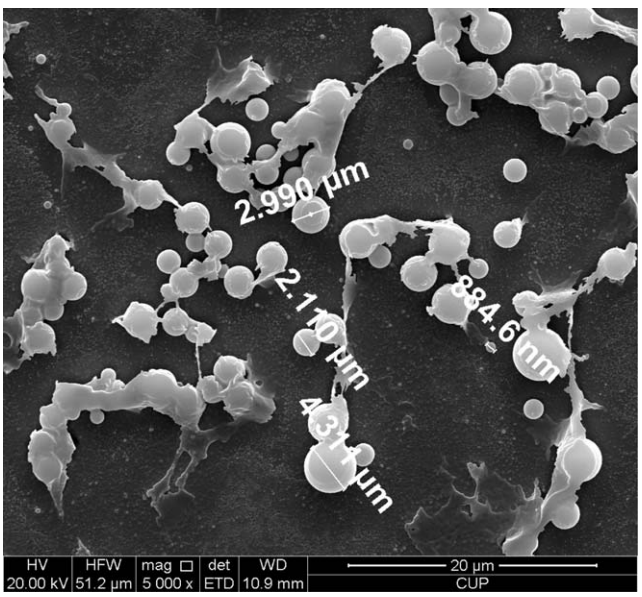

Figure 1. SEM image of CPAM emulsion.

EXPERIMENTAL

Reagents and Instruments

Span80, acrylamide, acrylic acid, anhydrous ethanol, N-pentane, and $NaHSO_3$ were all analytical reagents that were purchased from Beijing Yili Chemical Co., Ltd. Both $(NH_4)_2S_2O_8$ and methylene blue, were analytically pure and purchased from Ann Nike Ju Chemistry. The deionized water was filtered by a 0.22 mm cellulose acetate microporous membrane. The nuclear-pore membrane with a diameter of 1.2 μm and thickness of 10 μm was provided by the China Institute of Atomic Energy. The BX-41 optical microscope was purchased from Japanese Olympus Co. Industrial white oil, with a boiling range between 150 °C and 300 °C, was chosen as continuous phase.

Methods

Synthesis and Purification of Crosslinked Polyacrylamide Microspheres. A certain amount of Span-80 and Tween-60 was dissolved in white oil as the oil phase, and acrylamide, acrylic acid, sodium hydroxide, and the crosslinking monomers were dissolved in water as the aqueous phase. Then, the two phases were mixed to form a W/O emulsion. With regards to oxidation of the reduction system, $(NH_4)_2S_2O_8$-$NaHSO_3$, was used to initiate system polymerization with a temperature increase from 22 °C to 70 °C. The reagents reacted isothermally for two hours

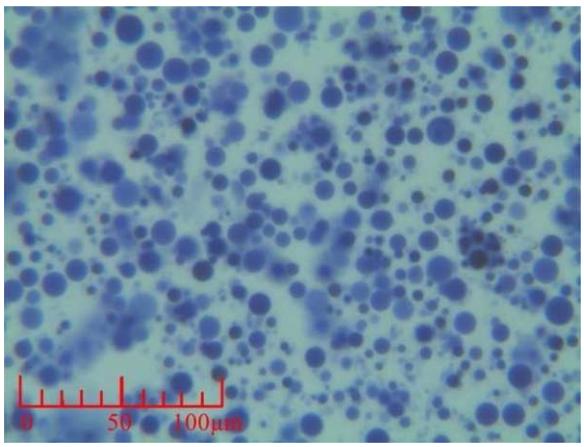

Figure 2. Microscopic image of 100 mg/L CPAM in water dispersion system after swollen for 5 days at 50 °C. [Color figure can be viewed in the online issue, which is available at wileyonlinelibrary.com.]

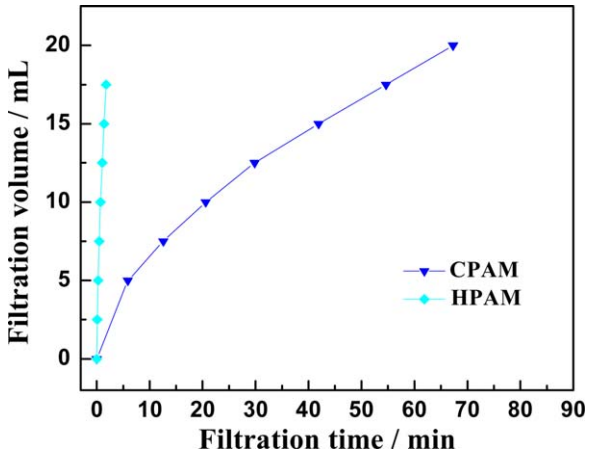

Figure 3. Filtration volume versus filtration time curves of the 100 mg/L CPAM system after swollen for 5 days at 50 °C and 100 mg/L HPAM solution under 50 kPa filtration pressure. [Color figure can be viewed in the online issue, which is available at wileyonlinelibrary.com.]

to afford an emulsion containing crosslinked polyacrylamide microspheres.

The emulsion with a volume ratio of 1:10 was dipped into anhydrous ethanol and fully stirred to facilitate demulsification, which generated much white flocculation sediments at the bottom of the container. The system was filtered to obtain a filter cake. Then, the cake was washed with ethanol with a volume ratio of 1:5. Upon filtering the cake, it was dried naturally. To remove the surfactant in the filter cake, the dried cake was pounded with a glass rod, placed into the previously prepared filter tube, and the tube mouth was sealed. The paper tube was placed in a Soxhlet extractor cable extractor and extracted with 240 mL of a pentane solution for 48 h. The treated crosslinked polyacrylamide microspheres were white powders.

Observation with Optical Microscopy. The liquid sample was dropped onto a glass slide and then covered with a cover glass, and then the conformation of crosslinked polyacrylamide microspheres was observed under the light microscope BX-41 produced by Japan Olympus company.

Observation with Scanning Electron Microscopy (SEM). A small amount of crosslinked polyacrylamide microsphere powder was placed on a clean glass slide, and gold was sprayed on the surface; the powdered sample was observed under a SEM Quanta 200F manufactured by the FEI company of the United States.

Nuclear-Pore Membrane Filtration. The device and method of nuclear-pore membrane filtration have been reported previously.[17,22] The filtration pressure of the crosslinked polyacrylamide microspheres through the nuclear-pore membrane was 50 kPa, and the time required to filter 20 mL of the crosslinked polyacrylamide microspheres was recorded. The nuclear-pore membrane (diameter of 1.2 μm, thickness of 10 μm, and pore density of $5 \times 10^6/cm^2$) was provided by the China Institute of Atomic Energy.

Sandpack Displacement Experiments. The device and method of the sandpack displacement experiment are reported in ref. 19. The sand-pack tube was 50 cm long, the flow rate of the water flooding and crosslinked polyacrylamide microspheres displacement was 0.40 mL/min, and the experimental temperature was 50 °C.

Parallel twin-tube oil displacement devices were used to investigate the vertical profile control property of crosslink polyacrylamide microspheres. The sandpack tube parameters are shown in Table I. The crude oil used in the experiment was Dagang oil, and the length of the sandpack tube was 30 cm. In the experimental process, both water flooding and the CPAM microspheres dispersion system were used for displacement. Furthermore, the sandpack tube was evacuated, and saturated water was used to measure the pore volume, porosity, permeability of the water phase, saturated oil, bound water preparation, and subsequent water displacement. When water was displaced, the pressure, the amounts of produced fluid, and produced oil were all recorded. After the water amount reached 98%, and according to the requirements, a certain microsphere dispersion system slug was injected. Then, water flooding followed to calculate the plugging efficiency and the recovery efficiency.

Micro-Visual Model. A 500 mg/L crosslinked polyacrylamide microsphere solution was injected into the micro-visual model using a constant-flux pump, and optical microscopy was used to observe the oil–water distribution when the CPAM microspheres flowed into the model to evaluate the areal sweep of the crosslinked polyacrylamide microspheres.

RESULTS AND DISCUSSION

Swelling Properties of Crosslinked Polyacrylamide Microspheres

Figure 1 is a SEM image of the micro crosslinked polyacrylamide microspheres emulsion. The microspheres were spherical. Furthermore, the primary particle sizes of the crosslinked polyacrylamide microspheres were not homogenously distributed (from several hundreds of nanometers to 5 μm).

The primary particle sizes of the SEM-observed microsphere powder samples are the sizes when the microspheres are not swollen. However, when used for in-depth profile control and displacement, the crosslinked polyacrylamide microspheres were dispersed in water and became swollen, leading to particle sizes that were obviously different from those of the microsphere powder samples. Figure 2 shows the morphologies and particle sizes of crosslinked polyacrylamide microspheres at a concentration of 100 mg/L that were dispersed in deionized water and observed by SEM. It can be seen that the crosslinked polyacrylamide microspheres were regular spheres after they were dispersed in water. The particle size distribution was relatively wide and ranged from several hundreds of nanometers to approximately 18 μm. Compared with the primary particle sizes, the particle sizes of the swollen microspheres were approximately five times larger. This indicates that the crosslinked polyacrylamide microspheres had good swelling properties in water. The particle sizes of the microspheres in the dispersion

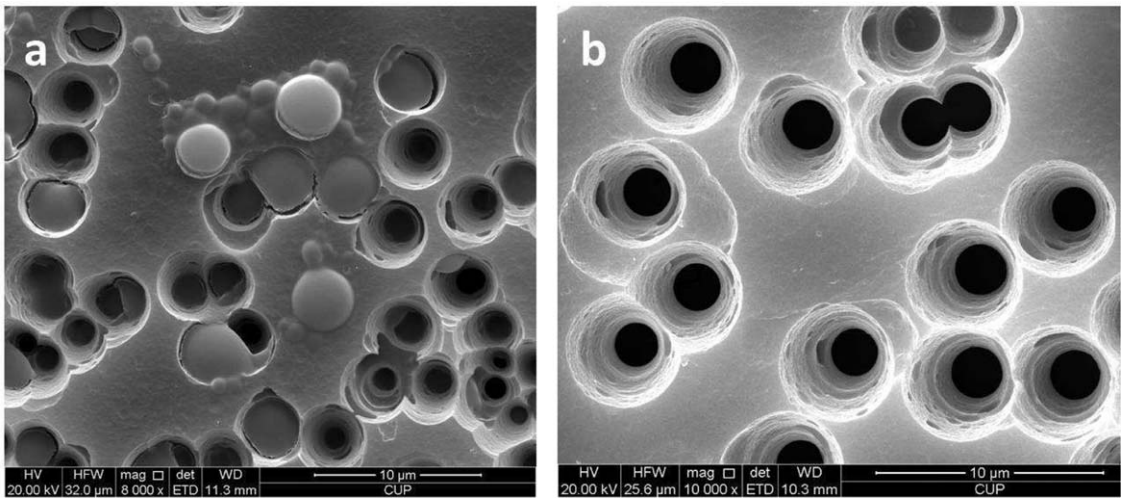

Figure 4. SEM photos of nuclear-pore membrane penetrated by the CPAM microspheres dispersed system (**a**) and HPAM solution (**b**).

system were not homogeneous and displayed a certain level of polydispersity, which was caused by the random distribution of crosslinking points during the polymerization process and the random array of —$CONH_2$ and —COONa in the molecular interior.

Plugging Properties of Crosslinked Polyacrylamide Microspheres

In the experimental process of microporous membrane filtration, the microporous membrane is regarded as a cross-section of the porous media, which can simulate the blocking effect of displaced fluid in the porous media. The interception mechanism of a microporous membrane is different due to its shape, size, structure, surface gravity, and deformation capability. Figure 3 shows the relationship between filtration volume and filtration time when 100 mg/L CPAM microspheres (underwent swelling at 50 °C for 5 days) and a dilute solution of HPAM of the same concentration were passed through a 1.2 μm nuclear-pore membrane. The relationship between the filtration volume and the filtration time of the polyacrylamide solution were found to be linear, and the filtration rate was too fast to block the nuclear-pore membrane. In contrast, the filtration curve of the crosslinked polyacrylamide microsphere dispersion system of the same concentration was a downward parabola, and its flow rate gradually decreased, indicating that CPAM microspheres could effectively block a nuclear-pore membrane with a pore diameter of 1.2 μm. The superior plugging properties of the crosslinked polyacrylamide microspheres compared with those of HPAM could be attributed to their different structures. For instance, in a partially hydrolyzed polyacrylamide solution, the molecular morphology of HPAM was a random coil that could be stretched and varied with the streamline. Furthermore, this morphology could easily become linear as a result of the flow shear tension under a given amount of pressure, thus causing HPAM to more rapidly penetrate the nuclear-pore membrane. The rapid flow makes the formation of a bridge between the HPAM molecules difficult, so effective blockage of the nuclear-pore membrane was not achieved. However, in a

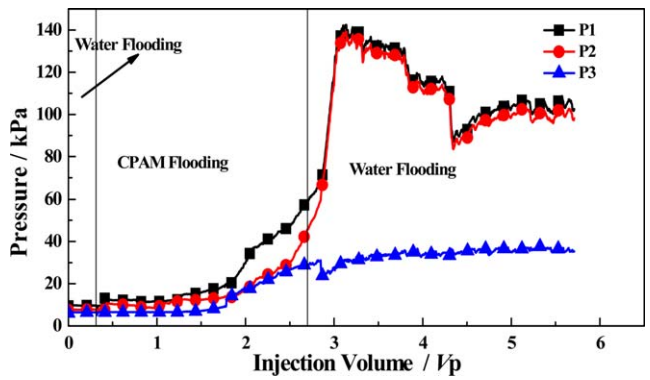

Figure 5. Relationship between the injection pressure and injection volume of 600 mg/L CPAM system after swollen for 5 days at 50 °C. The NaCl concentration is 5000 mg/L and the water permeability is 1.34 μm^2. [Color figure can be viewed in the online issue, which is available at wileyonlinelibrary.com.]

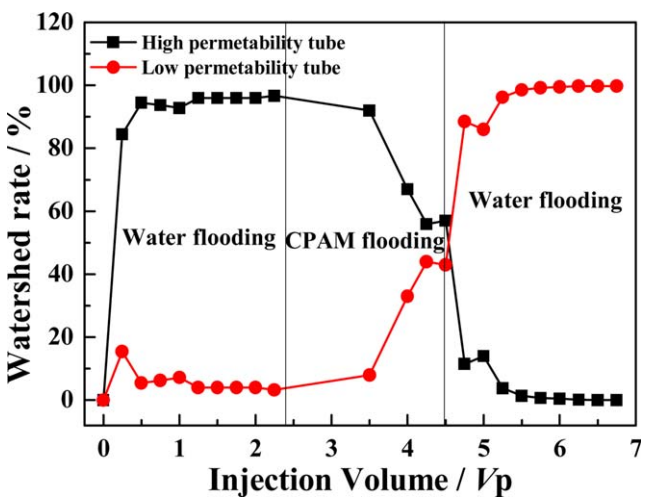

Figure 6. Relationship between the watershed rate of parallel twin-tube displacement and injection volume. The CPAM concentration is 600 mg/L and has been swollen for 5 days at 50 °C. The NaCl concentration is 5000 mg/L. [Color figure can be viewed in the online issue, which is available at wileyonlinelibrary.com.]

Figure 7. Appearance of ground glass model after oil saturation. [Color figure can be viewed in the online issue, which is available at wileyonlinelibrary.com.]

Figure 8. Sweep area change of ground glass model after water flooding ends. [Color figure can be viewed in the online issue, which is available at wileyonlinelibrary.com.]

crosslinked polyacrylamide microsphere dispersion system, the microspheres were approximately spherical and there were crosslinking points that could greatly restrict morphological changes. Moreover, the average apparent hydrodynamic diameters of the swelled microspheres were close to the pore size of the nuclear-pore membrane. Thus, crosslinked polyacrylamide microspheres could more easily adsorb and be retained in a nuclear-pore membrane, and as a result, the flow resistance was greatly increased, which led to a greater plugging effect than that of the HPAM solution.

To further illustrate the plugging effect of the crosslinked polyacrylamide microspheres on the nuclear-pore membrane, SEM measurements were used to observe pore size variations of the HPAM solution and the CPAM microsphere dispersion system at the same concentration after they penetrated the 1.2 μm pores, as shown in Figure 4. The pores of the nuclear-pore membrane could be clearly observed after the HPAM solution passed through the nuclear-pore membrane; in contrast, no HPAM molecules were retained on the nuclear-pore membrane surface. However, after CPAM microspheres penetrated the nuclear-pore membrane, the membrane surface was left partially covered, and a portion of the CPAM microspheres blocked the internal micropores. In particular, when the particle sizes were similar to the pore size of the nuclear-pore membrane, the microspheres could easily pass through the nuclear pore membrane and block the internal micropores with a pressure effect. As a result, the filtration rate of CPAM microspheres through the nuclear-pore membrane obviously decreased, and the plugging effect of the nuclear-pore membrane was enhanced.

As used for in-depth profile control, the dispersion system of crosslinked polyacrylamide microspheres must be able to enter the deep part of an oil reservoir to effectively block the major channel; however, the nuclear-pore membrane filtration experiment can only illustrate that crosslinked polyacrylamide microspheres have certain plugging properties. Therefore, a 600 mg/L CPAM microspheres dispersion system was swelled at 50 °C for 5 days and injected into a sand packed tube with a permeability of 1.34 μm^2 (50 cm in length, three isometric pressure points) at a certain linear flow rate. Throughout the experiment, the pressure of the water flooding was initially stable, and then, the 2.5 Vp crosslinked polyacrylamide microsphere dispersion system was injected, and the water flooding was subsequently replaced. Figure 5 illustrates the relationship between injection pressure and injection volume at three different positions in the sandpack tube. After the water was injected, the pressure reached equilibrium. Then, the 600 mg/L CPAM dispersion system was injected and the pressure at the three different positions in the sandpack tube increased with an increase in injection volume of the CPAM microspheres dispersion system. After 2.5 Vp of the polyacrylamide microsphere dispersion system was injected, the first pressure (P1) close to the inlet end increased from approximate 10 to 50 kPa, the second pressure (P2) at the middle position increased from approximate 8 to 30 kPa, and the third pressure (P3) close to the outlet end increased from approximate 7 to 25 kPa. When water was injected, the pressures P1, P2, and P3 continued to rise with a slight fluctuation but finally remained at approximate 100, 90, and 35 kPa, respectively, and had high resistance coefficients and residual resistance coefficients. All of the above results indicate that the CPAM microspheres dispersion system had certain plugging effects on the sandpack tube.

And the system could also enter the deep part of the sand tube to form effective plugging, which played the role of in-depth profile control. The CPAM microspheres were first adsorbed, then accumulated, bridged, and blocked the pores, which were close to the inlet end and lead to an increase in the P1 pressure. Furthermore, as the injection volume of the polyacrylamide microspheres increased, more and more crosslinked polyacrylamide microspheres accumulated in the pore of the inlet end, so the pressure P1 increased rapidly. Moreover, because the particle size of the swelled CPAM microspheres was small and had certain deformation properties, they could be deformed to penetrate through the first measuring point and reach the second and third measurement points under certain pressure. Then, the polyacrylamide microspheres adsorbed, accumulated, bridged, and blocked the second and third locations, which resulted in the increase of the P2 and P3 pressures and the injection volumes. After the water was injected, the P1, P2, and P3 pressures continued to increase, which further indicated that the crosslinked polyacrylamide microspheres had good deformation capabilities and could enter the deep part of the oil reservoir by deformation under pressure. Thus, the CPAM microspheres dispersion system played the role of in-depth profile control.

Vertical Profile Control Property of Crosslink Polyacrylamide Microspheres

Parallel twin-tube oil displacement devices were adopted to investigate the oil displacement and profile control performance of the CPAM microspheres dispersion system. When water was displaced in the high permeability and low permeability twin-

Figure 9. Sweep area changes of ground glass model during injection of 600 mg/L CPAM μm microspheres after swollen for 5 days at 50 °C. [Color figure can be viewed in the online issue, which is available at wileyonlinelibrary.com.]

tube model, the oil displacement efficiencies were obviously different: that is, the recovery efficiency of the high permeability tube was 77%, which was significantly higher than that of the low permeability tube, and the total oil displacement efficiency was 56.5%. As mentioned previously, this phenomenon occurred because water mainly flowed into the high permeability tube of low flow resistance when the water was displaced. When the water flooding concluded, a 1.75 Vp CPAM microspheres dispersion system of 600 mg/L was injected. At this time, the total oil displacement efficiency of the twin-tube was 80.0%, and the oil displacement efficiency of the microsphere displacement increased by 23.5% compared with that of water flooding. After injecting the microsphere dispersion system, the increased oil displacement efficiency primarily resulted from the low permeability sandpack tube, which had an oil displacement efficiency of 82.2% (a 48.2% improvement). In contrast, the oil displacement efficiency of the high permeability tube was 77.6%, which was only a 0.6% improvement (as shown in Table I). This was because the microspheres dispersion system resulted in a plugging and profile control effect. The CPAM microspheres dispersion system was preferentially injected into the high permeability tube to block the large pores. While water was subsequently displaced, it was preferentially injected into the low permeability tube (Figure 6); thus, the residual oil in the low permeability tube was replaced. The twin-tube experiment demonstrates that the microspheres dispersion system has a more obvious plugging effect than that of the high permeability tube with a certain profile control and displacement effect.

Planar Profile Control Property of Crosslinked Polyacrylamide Microspheres

To illustrate the planar profile control mechanism of the microsphere dispersion system, a glass sandblasting simulation model was used to investigate variations in the sweep area of water flooding and displacement of the microsphere dispersion system. For the experiments, the model was prepared by bonding two pieces of sandblasting glass together (60 μm in total width).

During the experiment, vacuumed saturated oil (30% crude oil simulation oil) was used, and after the oil was saturated, the ground glass model formed a homogeneous oil region (Figure 7). Then, the water was displaced, and when the water flooding ended, the ground glass had clearly breakthrough of a high permeability channel (Figure 8). Figure 8 shows that when the oil was displaced by water in the ground glass model, as the planar permeability of the ground glass model was inhomogeneous, a wide water flooding channel formed in the center of the model. Moreover, there was still an unaffected oil region, which had low permeability. This indicated that water mainly flowed in the direction of smallest resistance. When the oil in the channel with the smallest resistance was replaced, then water was displaced continuously, and the sweep coefficient increased to a lesser extent.

After the water flooding concluded, 600 mg/L CPAM microspheres were injected. These CPAM microspheres preferentially entered the water channel of high permeability. In the channel, CPAM microspheres were absorbed on the surface of the hydrophilic quartz sand, and this retention on the surface led to the accumulation of subsequent microspheres due to intermolecular forces. Furthermore, the microsphere retention provided the possibility of bridging and plugging and increased the flow resistance of the microsphere dispersion system, thus causing the subsequent flooding to flow around. The flow around caused the fluid displacement to flow to the residual oil channel, which was unaffected by the original water flooding. As a result, the force balance of the oil hole was broken, which caused the residual oil to be dispelled from its original position. The residual oil then flowed to the unblocked and high permeability channel. Therefore, it was found that the microsphere dispersion system injection led to an expansion of the affected area (Figure 9), and it was also determined that the crude oil in the original water flooding channel was continuously displaced. Meanwhile, the residual oil in the area unaffected by the water flooding was expelled, so the sweep area and recovery efficiency both improved.

CONCLUSIONS

1. The morphology of the CPAM microspheres was spherical, with diameters that were between several hundreds of nanometers and 5 μm. After swollen in water, the microspheres retained their spherical morphologies, but the particle sizes increased by approximately five times of their original size.
2. CPAM microspheres were easily absorbed and retained in pores and effectively plugged the high permeability channel. As a result, a flow diversion effect occurred in the vertical and planar direction, which improved the involved coefficient and enhanced the recovery efficiency.
3. The CPAM microspheres had good deformation abilities. They could enter the deep part of an oil reservoir by deformation under pressure; thus, they functioned as an in-depth profile control in this study. They could displace the residual oil on the pore wall and water channel when they migrated in a porous medium, so the synchronous effect of profile control and coordination was achieved to improve the recovery efficiency.

ACKNOWLEDGMENTS

This research is supported by National Natural Science Foundation of China No.51274211 and Major National Science and Technology Projects (2011ZX05009).

REFERENCES

1. Al-Muntasheri, G. A.; Nasr-El-Din, H. A.; Al-Noaimi, K.; Zitha, P. L. *SPE J.* **2007**, *14*, 245.
2. Taylor, K.; Burke, R.; Nasr-El-Din, H.; Schramm, L. *J. Petrol. Sci. Eng.* **1998**, *21*, 129.
3. Xie, C.; Feng, Y.; Cao, W.; Teng, H.; Li, J.; Lu, Z. *J. Appl. Polym. Sci.* **2009**, *111*, 2527.
4. Bratby, J. Coagulation and Flocuulation; England: Uplands Press Croydon, **1980**.
5. Dentel, S. K.; Gucciardi, B. M.; Griskowitz, N. J.; Chang, L. L.; Raudenbush, D. L.; Arican, B. In Chemical Water and Wastewater Treatment VI; Springer, **2000**.

6. Peng, X.; Shen, J.; Xiao, H. *J. Appl. Polym. Sci.* **2006**, *101*, 359.
7. Arnold, C.; Wallace, A.; U.S. Patent Application No. 10/156, 313 2002-5-28.
8. Datla, N. V.; Koo, J. Y.; Choi, D. J.; Assari, S.; Hemmasizadeh, A.; Podder, T. K.; Dicker, Y. Y.; Darvish, A. P.; Hutapea, K. P. *J. Med. Devices* **2012**, *6*, 017599.
9. Nakashima, K.; Bahadur, P. *Adv. Colloid Interface Sci.* **2006**, *123*, 75.
10. Muller, G. *Polym. Bull.* **1981**, *5*, 31.
11. Yang, F.; Li, G.; He, Y. G.; Ren, F. X.; Wang, G. *Carbohydr. Polym.* **2009**, *78*, 95.
12. Kang, W. L.; Hu, L. L.; Zhang, X. F.; Yang, R. M.; Fan, H. M.; Geng, J. *Petrol. Sci.* **2015**, *12*, 483.
13. Liu, H.; Zhang, H.; Wang, S.; Wang, H.; Bao, S. *Pet. Sci.* **2006**, *3*, 51.
14. Zhao, F., China University of Petroleum Press, Dongying, **2006**.
15. Han, D. K.; Yang, C. Z.; Zhang, Z. Q.; Lou, Z. H.; Chang, Y. I. *J. Petrol. Sci. Eng.* **1999**, *22*, 181.
16. Xiong, S.; Liu, X.; Liu, W.; He, Y.; Ruan, X. *Petrol. Sci. Technol.* **2009**, *27*, 357.
17. Dawkins, J. V.; Gabbot, N. P.; Montenegro, A. M.; Lloyd, L. L.; Warner, F. P. *J. Chromatogr. A* **1986**, *371*, 283.
18. Junru, Y.; Xiaoqing, X.; Zhang, J.; Zheng, X.; Zhijie, W. *Petrol. Explor. Dev.* **2014**, *41*, 794.
19. Liu, Y. L.; Shen, J. W.; Li, G. H.; Zhang, G. C. *Adv. Mater. Res.* **2013**, *669*, 208.
20. Tian, Q. Y.; Wang, L.; Tang, Y.; Liu, C.; Ma, C.; Wang, T. SPE International Oilfield Nanotechnology Conference and Exhibition, **2012**.
21. Wang, L.; Zhang, G.; Li, G.; Zhang, J.; Ding, B. International Oil and Gas Conference and Exhibition in China, **2010**.
22. Zhang, P.; Dong, Y.; Huang, W.; Jia, Z.; Zhou, C.; Guo, M.; Yu, H. *J. Appl. Polym. Sci.* **2015**, *132*, DOI: 10.1002/app.42614.
23. Hua, Z.; Lin, M.; Dong, Z.; Li, M.; Zhang, G.; Yang, J. *J. Colloid Interface Sci.* **2014**, *424*, 67.
24. Hua, Z.; Lin, M.; Guo, J.; Xu, F.; Li, Z.; Li, M. *J. Petrol. Sci. Eng.* **2013**, *105*, 70.
25. Yao, C.; Lei, G.; Li, L.; Gao, X. *Energy Fuels* **2012**, *26*, 5092.
26. Yao, C.; Lei, G.; Hou, J.; Xu, X.; Wang, D.; Steenhuis, T. S. *Indus. Eng. Chem. Res.* **2015**, *54*, 10925.
27. Lin, M.; Zhang, G.; Hua, Z.; Zhao, Q.; Sun, F. *Colloids Surf. A* **2015**, *477*, 49.